Prepared for submission to JINST

19TH International Workshop on Radiation Imaging Detectors
2 – 6 July 2017
Krakow, Poland

Development and Characterization of a $4 \times 4\,\mathrm{mm}^2$ Pixel Neutron Scintillation Detector using Digital SiPMs

Matthias Herzkamp[a,1] **Daniel Durini**[a] **Carsten Degenhardt**[a] **Andreas Erven**[a] **Holger Nöldgen**[a] **Artem Feoktystov**[b] **Liubov Jokhovets**[a] **Matthias Streun**[a] **Andreas Schwaitzer**[c] **Stefan van Waasen**[a,d]

[a] *Central Institute of Engineering, Electronics and Analytics ZEA-2 – Electronic Systems, Forschungszentrum Jülich GmbH, D-52425 Jülich, Germany*

[b] *Jülich Centre for Neutron Science (JCNS) at Heinz Maier-Leibnitz Zentrum (MLZ), Forschungszentrum Jülich GmbH, Lichtenbergstr. 1, D-85748 Garching, Germany*

[c] *Central Institute of Engineering, Electronics and Analytics ZEA-1 – Engineering and Technology, Forschungszentrum Jülich GmbH, D-52425 Jülich, Germany*

[d] *University of Duisburg-Essen, Faculty of Engineering, Communication Systems (NTS), Bismarckstr. 81, 47057 Duisburg, Germany*

E-mail: m.herzkamp@fz-juelich.de

Abstract: This work describes the development of the first demonstrator device for neutron detection based on a ^{6}Li-glass as a scintillator and silicon photomultipliers (SiPM) as photodetector. For the first characterization, the scintillator was pixelated with a one to one correspondence between scintillator and SiPM pixels, and optical cross-talk between pixels was minimized. Measurements in a high luminosity neutron beam show the functionality of the device and allow for partial characterization. The position resolution is $4 \times 4\,\mathrm{mm}^2$ and the detection efficiency of neutrons is 91(6) % relative to the active area. The device is linear up to at least 600 kcps.

Keywords: Neutron detectors (cold, thermal neutrons), Scintillators, Photon detectors for visible photons (SiPMs)

[1]Corresponding author

Contents

1 Introduction

The world-wide shortage of ^{3}He has led to a search for alternative neutron detection methods. For thermal and cold neutrons, a popular possibility is the use of neutron scintillators like cerium doped Li-glass enriched in ^{6}Li in combination with a photodetector. A very popular choice for photodetectors in neutron detection applications are photomultiplier tubes (PMT, see e.g. [1, 2]). PMTs generally have good timing resolution and high photodetection efficiency, but they require high voltages and are sensitive to magnetic fields. Silicon photomultipliers (SiPM) reach similar efficiencies and timing resolution as PMTS, but have a lower operating voltage (tens of volts vs. kilovolts) and are insensitive to magnetic fields of up to several Tesla.

However, SiPMs have been largely ignored for neutron detection applications because of their vulnerability to neutron radiation damage. The main source of radiation damage in an environment rich in cold or thermal neutrons is the neutron capture and subsequent beta decay of ^{30}Si, which has an abundance of about 3 % in natural silicon:

$$^{30}\mathrm{Si} + n \longrightarrow {}^{31}\mathrm{Si} \longrightarrow {}^{31}\mathrm{P} + \beta \tag{1.1}$$

The resulting phosphorous acts as an electron donor in the silicon crystal, which effectively changes the dopant concentration. This reduces the lifetime of photogenerated charge carriers. Furthermore, it was reported [3], that each absorbed thermal or cold neutron causes two to five point defects in the silicon crystal lattice at room temperature. These two effects result in an increased dark count rate (DCR) and a decreased photon detection efficiency (PDE). Recently, the effects on the photodetection performance of SiPMs have been examined quantitatively. The results indicate, that with typical neutron dosages in small angle neutron scattering (SANS) experiments, a lifetime of up to 10 years can be expected [4].

2 Detector Concept

The detector consists of a scintillator which emits a light flash when capturing a neutron and an underlying photodetector sensing these light flashes. We use 1 mm thick cerium doped lithium glass GS20 from Scintacor [5] as scintillator. GS20 contains about 6.6 % lithium by weight, which is enriched in ^{6}Li to 95 %. A thermal or cold neutron has a high probability of reacting with ^{6}Li via

$$n + {}^6\mathrm{Li} \longrightarrow \alpha + {}^3\mathrm{H} + 4.78\,\mathrm{MeV}. \tag{2.1}$$

The energy released in this reaction is shared between the resulting alpha and triton particles only, which then traverse the lithium glass and ionize the material along their path. At the cerium impurities, the following de-excitation causes photons of 350 nm to 440 nm wavelength to be emitted isotropically.

The photodetector used is a Digital Photon Counter (DPC3200-22-44) from Philips (referred to as PDPC in the following). This device is a SiPM with digital readout of 3200 Single Photon Avalanche Diode (SPAD) cells with an active quenching circuit. The advantages of this approach are a simplified readout, mainly based on digital counting of avalanche events, a much lower time-jitter, and Correspondingly a better time resolution than that delivered by analog SiPMs.

A single PDPC tile is divided into a 4 × 4 array of so called dies, which are independent detection units operating a 2 × 2 pixel array each. This means that a tile consists of 64 pixels in an 8 × 8 array. The pixel size is about 3.2 × 3.8 mm^2, while the pixel pitch is 4 mm. This results in a fill factor of 76 % for each PDPC pixel.

Each die undergoes the readout cycle schematically shown in figure 1 independently. During the refresh phase, all SPAD cells are put into Geiger mode by increasing their voltage above the breakdown voltage. Then the die waits for a trigger, which can either be provided externally or caused by SPAD cell discharges.

After a configurable waiting period, the die checks if a validation condition is fulfilled in order to discriminate against triggers caused by thermally generated discharges or background events. If the condition is fulfilled, the die waits for a configurable integration period before reading out how many cells in each pixel were discharged, and refreshing all cells again.

The timestamp of each event is generated at the first trigger signal using a 9 bit Time to Digital Converter (TDC). Since the system runs on a 200 MHz clock, a timestamp quantum is 19.5 ps. This is a lower bound for the timing resolution of the system, which is not examined further in this work.

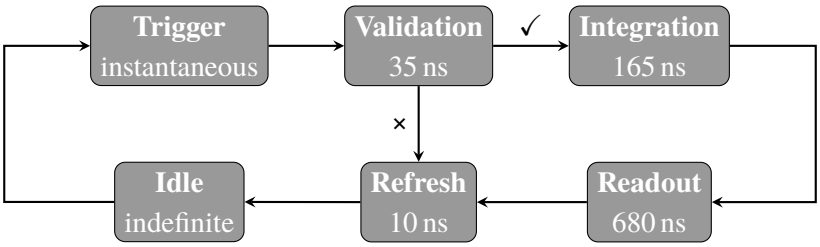

Figure 1. Diagram of the readout cycle of a PDPC die. Durations of validation and integration phases are configurable. Shown in this image are the values used during our measurements.

In order to examine the overall performance of the SiPM technology in neutron detection applications, the scintillator was divided into pixels to get a one to one correspondence between PDPC pixels and scintillator pixels. The pixels were created by cutting 700 µm deep, 300 µm wide grooves with a pitch of 4 mm into the 1 mm thick Li-glass. In order to reduce the optical cross-talk between the pixels, the grooves were filled with a white reflecting material containing TiO_2. The scintillator was directly glued to the 100 µm thick entrance window of the PDPC, with the grooves facing the PDPC. The other side of the scintillator was also painted white with TiO_2 in order to increase the amount of light impinging on the SiPM during a neutron event.

The PDPC module was cooled by a cooling system based on a Peltier element mounted on the backside of the module.

3 Test Measurements

We conducted first tests of our setup at the Kleinwinkel Streuanlage (KWS-1) instrument at the research neutron source Heinz Maier-Leibnitz (FRM II) [6]. As an instrument designed for Small Angle Neutron Scattering (SANS) experiments, the KWS-1 provides monochromatic neutrons with wavelengths ranging from 4.5 Å to 42 Å at high fluxes (up to $1 \times 10^8\,\mathrm{cm^{-2}\,s^{-1}}$). The flux can be adjusted by changing the collimation arperture, while the total intensity depends on the sample aperture. The detector installed at the KWS-1 is a $60 \times 60\,\mathrm{mm^2}$ Anger-camera [1] based on the same 1 mm thick GS20 scintillator as our demonstrator, and a 8 × 8 array of 7.6 cm diameter Photo Multiplier Tubes (PMT).

During the measurement we alternately placed our demonstrator in the beam to measure its response (see figure 2) and removed it again in order to measure the Anger-camera's response. After that, the neutron flux was increased by widening the collimation aperture and the measurement was repeated. The sample aperture was set to $2 \times 2\,\mathrm{mm^2}$, which ensured that even after some dispersion

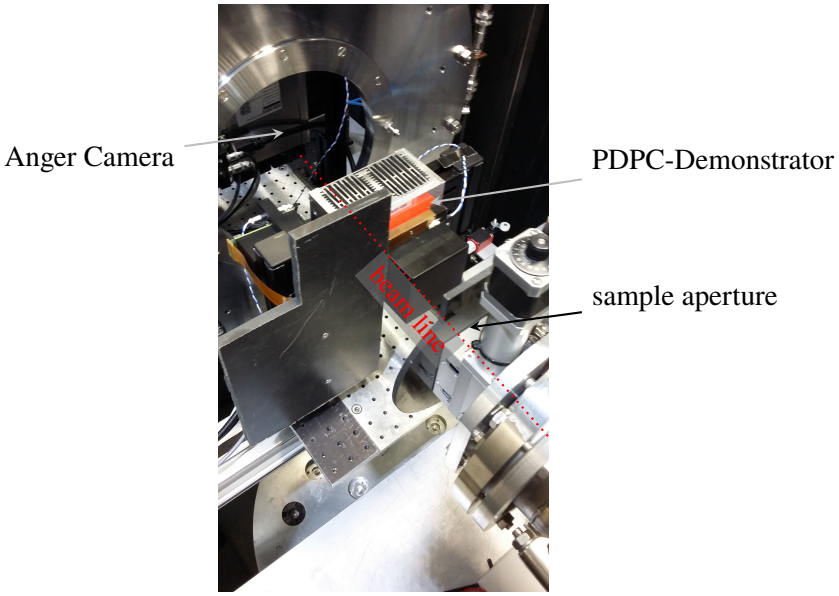

Figure 2. Photograph showing the position of the demonstrator device in the beam line.

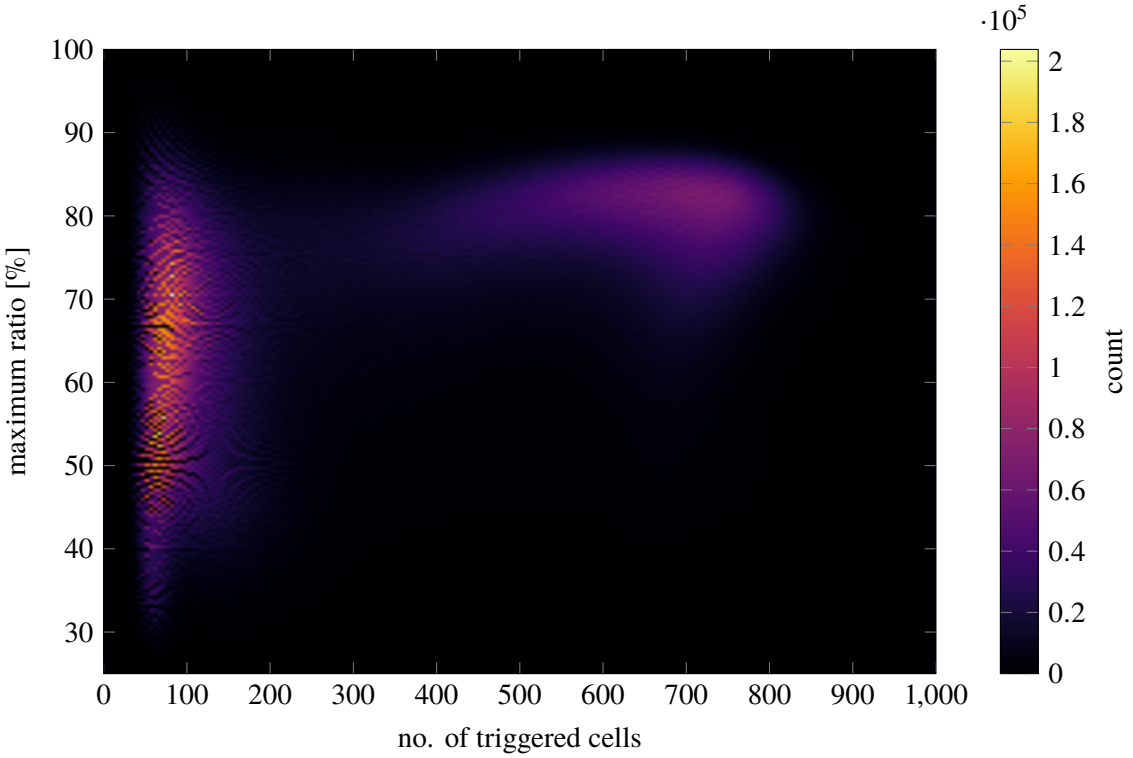

Figure 3. Histogram of maximum ratio defined in equation (4.1) versus total sum of triggered cells in a PDPC event, as measured by the demonstrator device during 60 min neutron exposure at the KWS-1.

due to the distance between aperture and detector, only one die of the PDPC was irradiated. Each Anger-camera and demonstrator measurement lasted 2 minutes

4 Results

A PDPC event is stored as the numbers $\{c_i\}_{i\in\{1,2,3,4\}}$ of triggered cells in each of the four pixels of a die. In case of a neutron event, the scintillation light should be restricted to a single SiPM pixel only, so one of the c_i should be greater than the rest. In order to quantify this, we define the maximum ratio of a photon event as

$$M = \frac{\max c_i}{\sum c_i}. \tag{4.1}$$

For aforementioned reasons, this value must be high for neutron events. Figure 3 shows a 2D histogram of the maximum ratio versus the total sum of triggered cells. It is filled with PDPC events recorded by the demonstrator device during a 60 min test measurement in presence of neutron radiation at the KWS-1. There are two main features visible in the plot. The one on the left contains events with low number of triggered cells and rather distributed maximum ratio, while the one on the right contains events with high number of triggered cells and high maximum ratio. In a control measurement without neutron radiation, the latter peak vanishes while the former remains. This

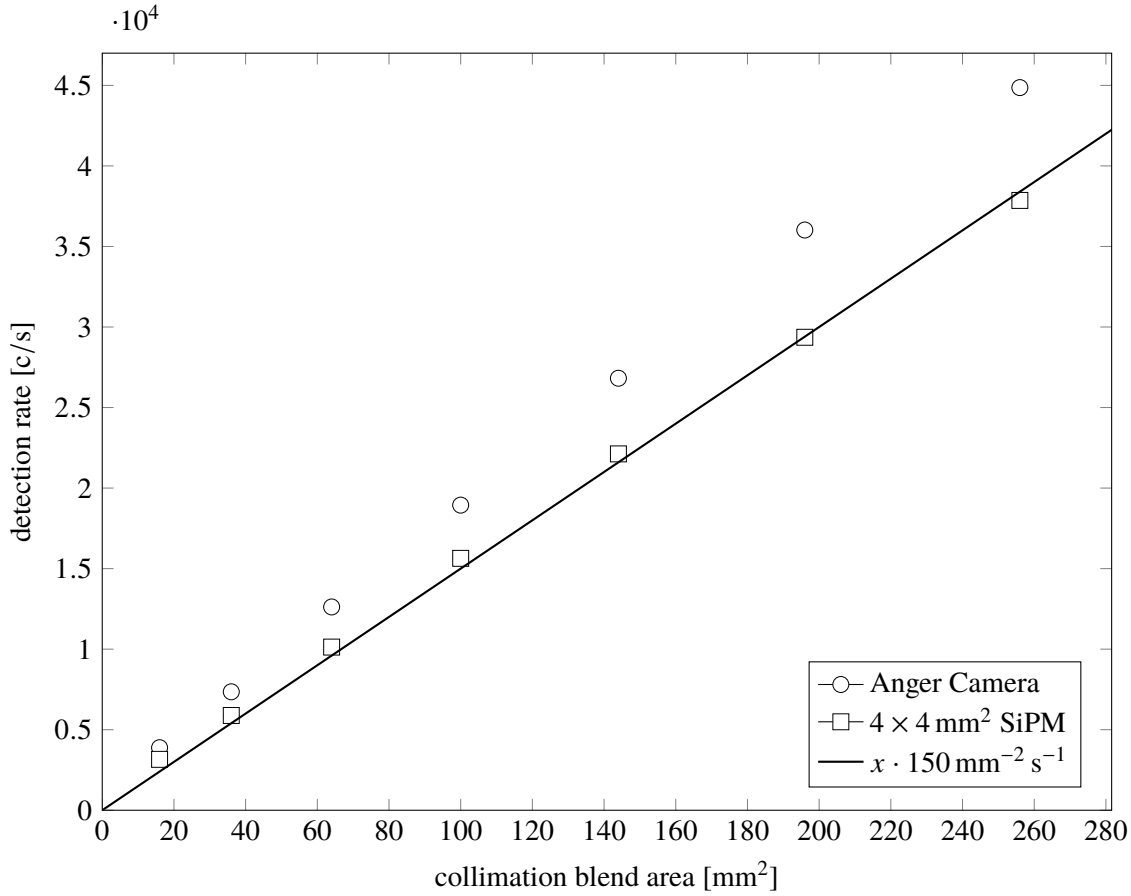

Figure 4. Detection rate of Anger-camera and demonstrator device dependent on collimation blend area. The line is a linear fit to the demonstrator device data.

identifies the neutron peak as the one with high number of triggered cells. The high maximum ratio of about 80 % for neutron events confirms that the supression of optical cross-talk works and is sufficient to determine the pixel in which the neutron event happened. Therefore the demonstrator has a position resolution of $4 \times 4\,\mathrm{mm}^2$.

Due to the clear separation of the peaks, it is simple to discriminate against the background signal by applying a selection threshold of 300 triggered cells. This way the demonstrator can be used as a neutron counter and its efficiency and linearity can be characterized and compared to that of the Anger-camera.

Figure 4 shows the detection rates of the Anger-camera and the demonstrator device respectively, obtained during measurements described in section 3. The linearity of both devices is evident for the measured interval of neutron fluxes. The maximum counting rate reached in this measurement reaches 40 000 cps, which can be interpreted as a lower bound in this context. Since only a single die was irradiated and since all dies work in parallel, the linearity scales with the number of dies, or with the area of the detector. Thus, relative to its area, the detector is linear up to about $600\,\mathrm{Mcps/m}^2$.

Averaged across different collimation settings, the demonstrator detection rate is about 83(5) % of the Anger-camera detection rate. Since both use the same type of scintillator and have the identical neutron source, they should be readily comparable. Much of the discrepancy can be explained by a geometrical reason: by inserting grooves into the demonstrator's scintillator, we effectively reduced the active area. With a groove width of 0.3 mm, each scintillator pixel has a size of $3.7 \times 3.7\,\mathrm{mm}^2 = 13.69\,\mathrm{mm}^2$, which is only 86 % of the $16\,\mathrm{mm}^2$ total area per pixel. Relating the detection rate to the active scintillator area gives us a demonstrator detection rate of 97(6) % of the Anger-camera detection rate. With an Anger-camera detection efficiency of 95 % [7], we can report a detection efficiency of 91(6) % for our demonstrator device.

5 Discussion and Outlook

In this work we described the development and test of a demonstrator device using SiPM technology in a neutron detector. We could demonstrate the functionality and perform a partial characterization. We found a position resolution of $4 \times 4\,\mathrm{mm}^2$, a detection efficiency of 91(6) % with respect to the active area of the scintillator, and a linearity up to at least 40 kcps per die or 600 $\mathrm{Mcps/m}^2$.

Beside the acquisition of events in the die, the data transmission rates and buffer sizes influence the linearity of the detector and introduce upper limits. Each die, for instance can only store 40 events per 2^{16} clock cycles, which amounts to about 120 000 events per seconds (with a 200 MHz clock). This limitation can be removed by using custom readout electronics and more powerful data transmission methods.

However, due to the SiPMs' vulnerability to neutron radiation, this kind of technology is not favourable for high flux applications, because the photodetector would deteriorate faster. The measured linearity is probably sufficient for all applications where SiPM is an option due to life time considerations.

The position resolution of $4 \times 4\,\mathrm{mm}^2$ is not the optimum. A principle similar to that fo the Anger-camera, where a neutron hit illuminates more than one pixel might yield a better resolution. To examine this, further PDPC tiles fitted with grooveless scintillators were tested as well during the measurements, and will be characterized in future work.

References

[1] G. Kemmerling, U. Bunten, U. Clemens, R. Engels, M. Heiderich, W. Pykhout-Hintzen, H. Rongen, J. Schelten, D. Schwahn, and K. Zwoll. Performance measurements of a new large-area neutron scintillation detector system. *IEEE Transactions on Nuclear Science*, 51(3):1098–1102, jun 2004.

[2] P. M. De Lurgio et al. 2-d scintillation position-sensitive neutron detector. In *IEEE Nuclear Science Symposium Conference Record, 2005*, volume 2, pages 648–653, Oct 2005.

[3] G.O. Fiori. Neutron transmutation doped silicon: lattice damage and characterization techniques. *Latin American Journal of Metallurgy and Materials*, 3(2):98–105, 1983.

[4] Daniel Durini et al. Evaluation of the dark signal performance of different SiPM-technologies under irradiation with cold neutrons. *Nucl. Instrum. Methods Phys. Res., Sect. A*, 835:99 – 109, 2016.

[5] (https://scintacor.com/products/6-lithium-glass/).

[6] Artem V. Feoktystov, Henrich Frielinghaus, Zhenyu Di, Sebastian Jaksch, Vitaliy Pipich, Marie-Sousai Appavou, Earl Babcock, Romuald Hanslik, Ralf Engels, Günther Kemmerling, Harald Kleines, Alexander Ioffe, Dieter Richter, and Thomas Brückel. KWS-1 high-resolution small-angle neutron scattering instrument at JCNS: current state. *Journal of Applied Crystallography*, 48(1):61–70, jan 2015.

[7] Henrich Frielinghaus, Artem Feoktystov, Ida Berts, and Gaetano Mangiapia. KWS-1: Small-angle scattering diffractometer. *Journal of large-scale research facilities JLSRF*, 1, aug 2015.